Electrochemistry of Dinuclear, Thiolate-Bridged Transition-Metal Compounds. 7.† Electrochemical Generation of Isomers of $[Mo_2Cp_2(CO)_2(\mu\text{-}SMe)_2]$ and Their Reactivity toward Isocyanide Ligands

Frédéric Gloaguen, Christine Le Floc'h,‡ François Y. Pétillon, and Jean Talarmin*

UA CNRS 322 "Chimie, Photochimie et Electrochimie Moléculaires", Université de Bretagne Occidentale, 29287 Brest Cédex, France

Moulay El Khalifa and Jean-Yves Saillard

UA CNRS 254 "Chimie du Solide et Inorganique Moléculaire", Université de Rennes I, 35042 Rennes Cédex, France

Received October 9, 1990

The electrochemical reduction of Mo(III) dinuclear thiolato complexes, e.g. $[Mo_2Cp_2(CO)_2(\mu\text{-}SMe)_3]^+$ (1) and $[Mo_2Cp_2(CO)_2(X)_2(\mu\text{-}SMe)_2]$ (X = Cl (2), X = Br (3)), leads to a common product, *trans*-$[Mo_2Cp_2(CO)_2(\mu\text{-}SMe)_2]$, via a common intermediate that is a kinetic isomer of the stable product. EHMO calculations carried out on the model $[Mo_2Cp_2(CO)_2(\mu\text{-}SH)_3]^+$ are consistent with the proposed nature of the intermediate. The CO-catalyzed isomerization of the intermediate, the reactivity of both isomers of $[Mo_2Cp_2(CO)_2(\mu\text{-}SMe)_2]$ toward isocyanide ligands RNC (R = *t*-Bu, Bz, xyl), and the CO-induced isomerization of the resulting products $[Mo_2Cp_2(CO)(CNR)(\mu\text{-}SMe)_2]$ are reported.

Introduction

The chemistry and electrochemistry of di- and polynuclear metal complexes with sulfide or thiolate bridges have been under intensive scrutiny for several years.[1-3] Part of this interest arises from the implication of such species in biological[4,5] or catalytic[6] processes.

Although they are much simpler than the compounds involved in natural processes, dinuclear complexes possessing a $M_2(\mu\text{-}S)_n$ or $M_2(\mu\text{-}SR)_n$ core are of interest since they give rise to a rich chemistry that can be regarded as a model for catalytic or enzyme-driven reactions.[7,8]

Previous reports from this laboratory described the electrochemistry of simple dinuclear carbonyl complexes possessing -SR bridges. A variety of chemical reactions resulted from the electrochemical activation of $[Mo_2Cp_2(CO)_4(\mu\text{-}SR)_2]^{0/2+}$ such as oxidatively induced trans/cis isomerization[9] and oxidatively induced and electron-transfer-catalyzed substitutions of MeCN or *t*-BuNC for CO.[10]

We now report on the electrochemical activation of dimolybdenum(III) compounds, derived from *cis*-$[Mo_2Cp_2(CO)_4(\mu\text{-}SMe)_2]^{2+}$ by substitution of two carbonyls by a bridging methanethiolate or by two halide ligands. The synthesis of these compounds, $[Mo_2Cp_2(CO)_2(\mu\text{-}SMe)_3]^+$ (1), $[Mo_2Cp_2(CO)_2(X)_2(\mu\text{-}SMe)_2]$ (X = Cl (2), X = Br (3)) has been reported previously.[11] The reduction of 1-3 produces a reactive site that can interact with CO and isocyanide ligands. The reactions of this intermediate and of its stable isomer *trans*-$[Mo_2Cp_2(CO)_2(\mu\text{-}SMe)_2]$ with RNC lead to isomeric forms of a new complex $[Mo_2Cp_2(CO)(CNR)(\mu\text{-}SMe)_2]$. A preliminary account of this work has already been reported.[12]

Results and Discussion

I. Electrochemical Generation of a Reactive Intermediate. The cyclic voltammetry of complexes 1 and 3 is illustrated in Figures 1 and 2, and the potentials of the primary redox processes are listed in Table I. Although the oxidation of the complexes has not been investigated in detail, the first oxidation step is shown in the figures since it has been used as an internal standard for a reversible, diffusion-controlled one-electron transfer.[13]

1. Reductive Cleavage of Mo-X Bonds from 2 and 3. The reduction part of the cyclic voltammetry (CV) of 2 and 3 appears qualitatively similar in thf or MeCN electrolytes: an irreversible two-electron reduction (by comparison of $i_{p,red1}$ to $i_{p,ox1}$; $i_{p,red1}$ and $i_{p,ox1}$ are the peak currents for the primary reduction and oxidation steps, respectively) is followed by two reversible one-electron couples at more negative potentials (Figure 1 and Table I). The latter, as well as the oxidation peak detected on the reverse scan ($E_{p,ox}$ = -0.12 V in thf, -0.22 V in MeCN, Table I), is due to the redox processes of a *common intermediate* arising from the reductive cleavage of both

† For part 6, see ref 12.

‡ Present address: AFRC Institute of Plant Science Research, Nitrogen Fixation Laboratory, University of Sussex, Brighton BN19RQ, England.

(1) Wachter, J. *J. Coord. Chem.* **1987**, *15*, 219 and references therein.
(2) Blower, P. J.; Dilworth, J. R. *Coord. Chem. Rev.* **1987**, *76*, 121 and references therein.
(3) Zanello, P. *Coord. Chem. Rev.* **1988**, *83*, 199 and references therein.
(4) Holm, R. H. *Chem. Soc. Rev.* **1981**, *10*, 455.
(5) Burgmayer, S. J. N.; Stiefel, E. I. *J. Chem. Educ.* **1985**, *62*, 943.
(6) Chianelli, R. R. *Catal. Rev.-Sci. Eng.* **1984**, *26*, 361.
(7) Rakowski-Dubois, M. *Chem. Rev.* **1989**, *89*, 1.
(8) Bernatis, P.; Laurie, J. C. V.; Rakowski-Dubois, M. *Organometallics* **1990**, *9*, 1607.
(9) Courtot-Coupez, J.; Guéguen, M.; Guerchais, J. E.; Pétillon, F. Y.; Talarmin, J.; Mercier, R. *J. Organomet. Chem.* **1986**, *312*, 81.
(10) El Khalifa, M.; Guéguen, M.; Mercier, R.; Pétillon, F. Y.; Saillard, J. Y.; Talarmin, J. *Organometallics* **1989**, *8*, 140.
(11) Gomes de Lima, M. B.; Guerchais, J. E.; Mercier, R.; Pétillon, F. Y. *Organometallics* **1986**, *5*, 1952.
(12) Le Floc'h, C.; Pétillon, F. Y.; Pickett, C. J.; Talarmin, J. *J. Organomet. Chem.* **1990**, *390*, C39.
(13) The primary oxidation peak current ($i_{p,ox1}$) for 1 and 3 are comparable, under the same conditions of concentration, to $i_{p,ox1}$ for $[Fe_2Cp_2(CO)_2(\mu\text{-}SMe)_2]$, which was shown[14-16] to undergo an uncomplicated one-electron oxidation.
(14) Dessy, R. E.; Stary, F. E.; King, R. B.; Waldrop, M. *J. Am. Chem. Soc.* **1966**, *88*, 471.
(15) Frisch, P. D.; Lloyd, M. K.; Mc Cleverty, J. A.; Seddon, D. *J. Chem. Soc., Dalton Trans.* **1973**, 2268.
(16) De Beer, J. A.; Haines, R. J.; Greatex, R.; Van Wyk, J. A. *J. Chem. Soc., Dalton Trans.* **1973**, 2341.

0276-7333/91/2310-2004$02.50/0

Table I. Primary Redox Processes of Complexes 1–3 and Detection Potentials of the Electrogenerated Intermediate I[a]

		primary redox processes		intermediate I		
complex	solvent	$E_{p,red1}$, V	$E^{1/2}_{ox1}$, V	$E^{1/2}_{red1}$, V	$E^{1/2}_{red2}$, V	$E_{p,ox}$ ($E_{p/2}$), V
1	thf	−1.57	+0.67	−1.90	−2.47	−0.12 (−0.18)
	MeCN	−1.47 ($E^{1/2}$)	+0.72	−1.77	−2.19	−0.23 (−0.30)
	CH_2Cl_2	−1.60	+0.80	−1.87	−2.36 (irr)	−0.07 (−0.15)
2	thf	−1.79	+0.23	−1.89	−2.47	−0.12 (−0.21)
	MeCN	−1.65	+0.29 (−30 °C)	−1.78	−2.20	−0.22 (−0.31)
	CH_2Cl_2	−1.77	+0.28	−1.87	−2.37 (irr)	−0.09 (−0.17)
3	thf	−1.70	+0.20	−1.90	−2.47	−0.12 (−0.21)
	MeCN	−1.59	+0.27	−1.78	−2.20	−0.21 (−0.29)
	CH_2Cl_2	−1.68	+0.27	−1.86	−2.37 (irr)	−0.09 (−0.19)

[a] From cyclic voltammetry, v = 0.2 V s^{-1}.

Scheme I[a]

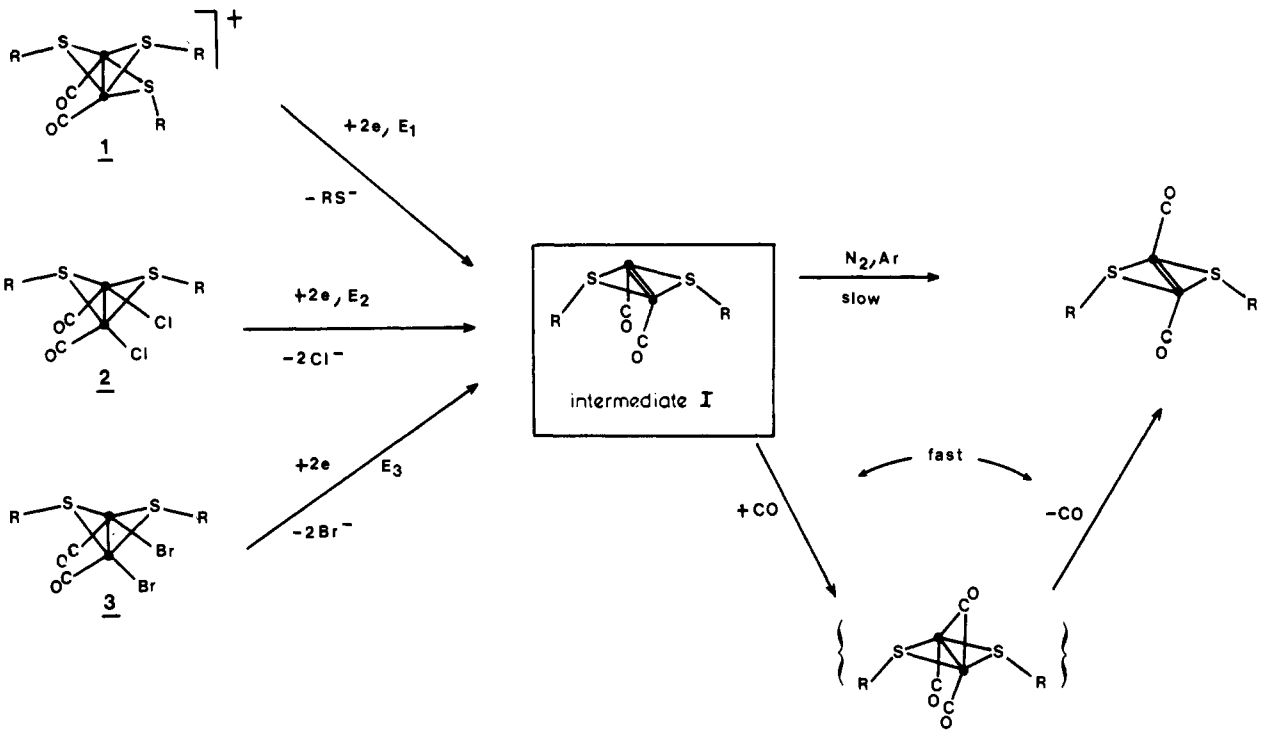

[a] ● = Mo–Cp. R = Me.

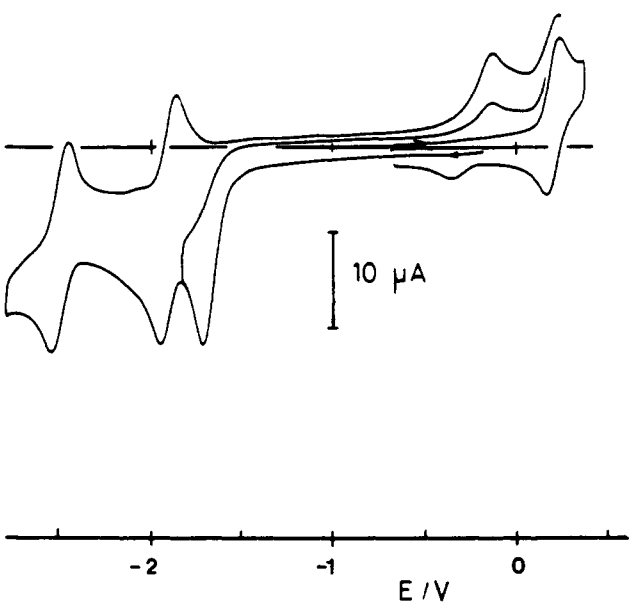

Figure 1. Cyclic voltammetry of a 0.4 mM solution of $[Mo_2Cp_2(CO)_2(Br)_2(\mu\text{-}SMe)_2]$ (3) in thf-Bu_4NPF_6 (vitreous carbon electrode; scan rate 0.2 V s^{-1}.

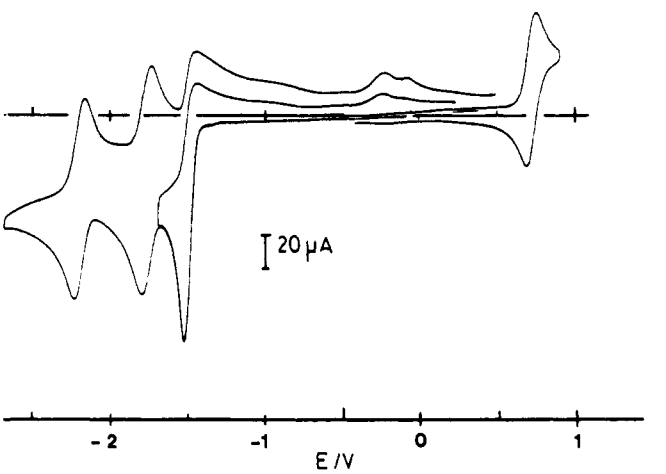

Figure 2. Cyclic voltammetry of a 1.65 mM solution of $[Mo_2Cp_2(CO)_2(\mu\text{-}SMe)_3]^+$ (1) in MeCN–0.1 M Bu_4NPF_6 (vitreous carbon electrode; scan rate 0.2 V s^{-1}.

Mo–X bonds at $E_{p,red1}$. The nature of the common intermediate (intermediate I, Scheme I) will be discussed in more detail in section I.3. Controlled-potential electrolyses of both 2 and 3 performed at $E_{p,red1}$ under an inert atmo-

Scheme II

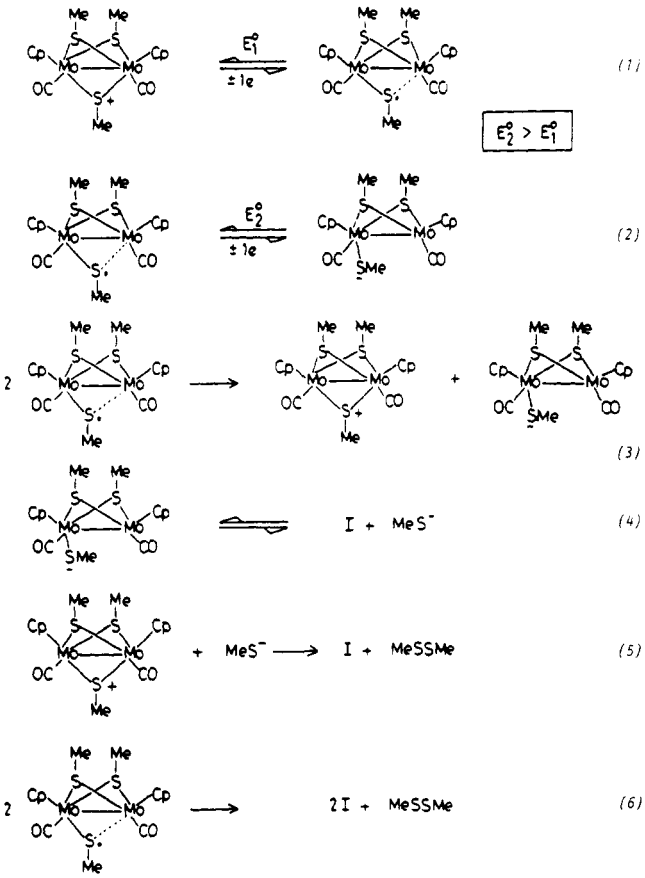

sphere lead to the product *trans*-$[Mo_2Cp_2(CO)_2(\mu\text{-}SMe)_2]$[17] in almost quantitative yield after consumption of ca. 2 F/mol of starting material (reaction 1). This process is

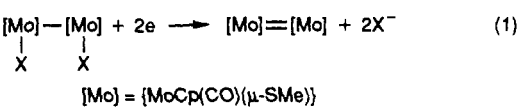

analogous to the electrochemical generation of the carbon–carbon double bond from organic *vic* dihalides,[19] reaction 2.

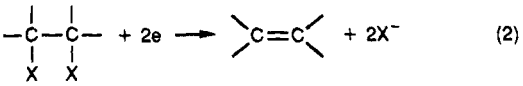

2. Reductive Cleavage of One -SMe Bridge from 1. The reduction mechanism of 1 is more complex than that for **2** or **3**, due to the reactivity of the thiolate ion or radical. However, the CV in Figure 2 demonstrates that the primary reduction of 1 leads to the same intermediate as those of **2** and **3** (Table I): it can therefore be concluded that the reduction at $E_{p,red1}$ results in the loss of one thiolate bridge (Scheme I). In agreement with the findings of section I.1, controlled-potential electrolyses of 1 at $E_{p,red1}$ at room temperature or at −20 °C (MeCN electrolyte, inert atmosphere) produce *trans*-$[Mo_2Cp_2(CO)_2(\mu\text{-}SMe)_2]$ almost quantitatively (vide infra).

The primary reduction of 1 is a partially reversible, diffusion-controlled, two-electron (by comparison of $i_{p,red1}$ to $i_{p,ox1}$) process in a MeCN electrolyte (Figure 2). The reversible transfer of two electrons in a single step requires that the second transfer (E°_2) be easier than the first one (E°_1), i.e. for a reduction $E^\circ_2 > E^\circ_1$ (Scheme II, steps 1 and 2). Under these conditions, the product resulting from the first electron transfer disproportionates (Scheme II, step 3). This type of ECE process has already been met in the case of the $[Mo_2Cp_2(CO)_3(L)(\mu\text{-}SR)_2]^{0/2+}$ couples (L = CO, *t*-BuNC; R = Me, Ph): the chemical step triggering the transfer of the second electron was assigned to a modification of the core geometry.[20]

In the present case, we believe that the chemical step (C_1) responsible for the EC_1E process involves a modification of one of the Mo–S bonds of the third thiolate bridge.

As shown by the scan rate dependence of the anodic to cathodic peak current ratio for the primary reduction ($(i_p^a/i_p^c)_{red1} < 1$; $(i_p^a/i_p^c)_{red1}$ decreases with increasing scan rates), a reversible chemical reaction C_2 is also coupled after the electron-transfer steps.[21] The chemical step C_2, resulting in the formation of the intermediate I, is assigned

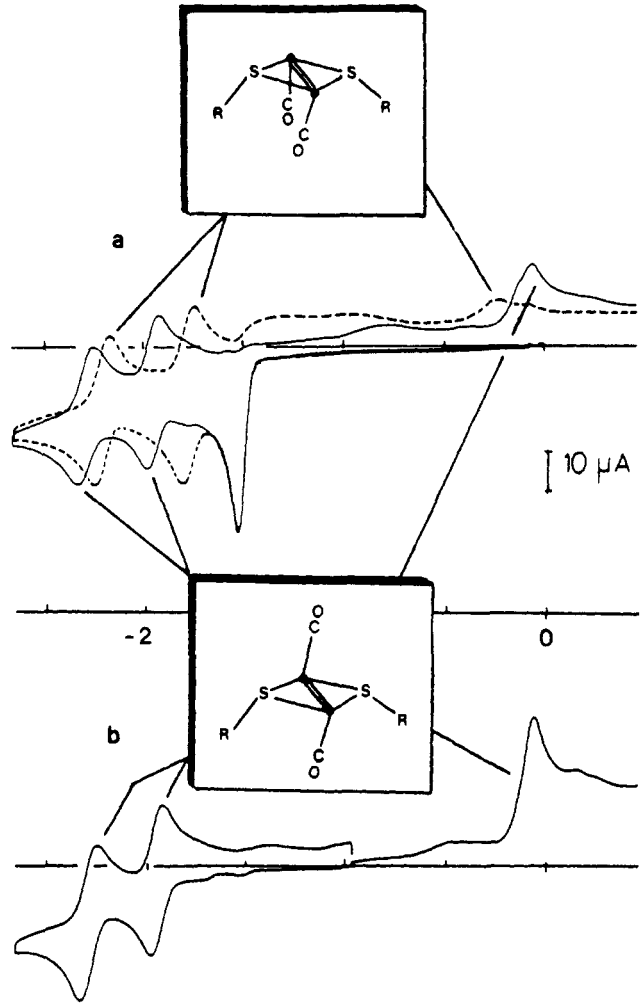

Figure 3. Cyclic voltammetry of a 0.8 mM solution of $[Mo_2Cp_2(CO)_2(\mu\text{-}SMe)_3]^+$ (1) (a) under N_2 (---) and under CO (—) and (b) after electrolysis at −1.6 V under Ar at a Hg-pool cathode (CV under Ar) (MeCN–0.1 M Bu_4NPF_6; vitreous carbon electrode; scan rate 0.2 V s^{-1}).

(17) *trans*-$[Mo_2Cp_2(CO)_2(\mu\text{-}SMe)_2]$ was identified from IR, ^1H NMR, and mass spectra after extraction from the catholyte. The assignment was confirmed by the comparison of the redox potentials of the product with those of an authentic sample prepared by an independent route.[18]

(18) Le Quéré, J. L. Thesis, Brest, 1982.

(19) Tallec, A. *Electrochimie Organique–Synthèse et Mécanismes*; Masson: Paris, 1985.

(20) Guéguen, M.; Pétillon, F. Y.; Talarmin, J. *Organometallics* **1989**, *8*, 148.

(21) Brown, E. R.; Large, R. F. In *Techniques of Chemistry*; Weissberger, A., Rossiter, B. W. Eds.; Wiley: New York, 1971; Vol. 1, Part IIA, pp 423–530.

Table II. Coulometric Results from Controlled-Potential Electrolyses of 1-3 at $E_{p,red1}$ under an Inert Atmosphere (Hg Pool Cathode)

complex	concn, M	solvent	*n*, F/mol	yield[a] of *trans*-$[Mo_2Cp_2(CO)_2(\mu\text{-}SMe)_2]$, %
1	2.7×10^{-4}	MeCN	1.90	93
	7.0×10^{-4}		1.74	96
	1.0×10^{-3}		1.45	96
	1.7×10^{-3}		1.59	95
	2.6×10^{-3}		1.59	93
	6.1×10^{-3}		1.50	100
1	4×10^{-4}–1.2×10^{-3}	thf	1.3	ca. 97
2	8×10^{-4}–6×10^{-3}	thf CH_2Cl_2 MeCN	1.9	ca. 100
3				

[a] Calculated by comparison of the oxidation peak current of the starting material before electrolysis to the first reduction peak current of the product *trans*-$[Mo_2Cp_2(CO)_2(\mu\text{-}SMe)_2]$ (see Experimental Section).

to the reversible loss of SMe^- from the anionic dinuclear complex (Scheme II, step 4).

In addition to the reactions detected by CV (Scheme II, steps 1–4) others take place on the longer time scale of electrolyses that produce *trans*-$[Mo_2Cp_2(CO)_2(\mu\text{-}SMe)_2]$ almost quantitatively (Figure 3b). In a MeCN electrolyte, the dependence of the coulometric *n* value on the experimental conditions (Table II) suggests that coupling reactions are involved. One such reaction was evidenced by adding $[Et_4N][SMe]$ to 1: the severe suppression of the primary reduction peak demonstrates that 1 is attacked by SMe^- (Scheme II, step 5).

The electrolyses of 1 performed in a thf medium under N_2 also produce *trans*-$[Mo_2Cp_2(CO)_2(\mu\text{-}SMe)_2]$ quantitatively, after consumption of only 1.3 F/mol of 1 (Table II). Although the reduction mechanism of 1 was not investigated in detail in this solvent, it appears that step 5 (Scheme II) must contribute significantly to the overall reduction process.

The last step in Scheme II results from the combination of steps 3–5.

3. Nature of the Intermediate I. The electrochemical generation of the intermediate I from the reduction of the dicarbonyl complexes 1–3 under N_2 or Ar in thf, MeCN, and CH_2Cl_2 electrolytes and the quantitative conversion of I into *trans*-$[Mo_2Cp_2(CO)_2(\mu\text{-}SMe)_2]$ on the CPE time scale (Figure 3a (broken line), b) have several implications: (i) the intermediate I does not contain halide ligands or three SMe bridges; (ii) I retains the $[Mo_2Cp_2(CO)_2(\mu\text{-}SMe)_2]$ assembly of its precursors and of the stable product; (iii) solvent molecules are not involved as ligands in I, as indicated by the similar redox potentials measured in solvents possessing different coordinating abilities such as thf and CH_2Cl_2 (Table I). All these facts concur to establish that the intermediate is a kinetically favored isomer of *trans*-$[Mo_2Cp_2(CO)_2(\mu\text{-}SMe)_2]$.

Two types of isomerism must be considered on the basis of the relative arrangement of the Cp and CO ligands (cis/trans isomerism) and/or due to the mutual orientation of the methyl groups on the bridging S atoms (syn/anti isomerism). Our reasons for attributing the cis geometry to the intermediate (Scheme I) are as follows.

(i) The electronic structure of one of the starting materials of the reactions of Scheme I, namely $[Mo_2Cp_2(CO)_2(\mu\text{-}SMe)_3]^+$ (1), has been investigated by extended Hückel molecular orbital (EHMO) calculations. This cation has been structurally characterized in its cis conformation.[11] From the EH calculations performed[22] on the model $[Mo_2Cp_2(CO)_2(\mu\text{-}SH)_3]^+$, the trans conformation appears highly disfavored, mainly for steric reasons. A comparison of the Mo–S overlap populations indicates that the SH group situated on the same side of the Mo–Mo bond as the Cp ligands is slightly less strongly bonded than the other two thiolato ligands (corresponding values: 0.40 vs 0.44). Moreover, the LUMO, which can be identified as the σ^*(Mo–Mo) orbital is somewhat antibonding between this peculiar sulfur and the metal atoms. These results support the proposition of the first steps of Schemes I and II: the starting compound $[Mo_2Cp_2(CO)_2(\mu\text{-}SMe)_3]^+$, which is probably in the cis conformation, loses upon reduction the thiolato group that lies on the Cp side, generating *cis*-$[Mo_2Cp_2(CO)_2(\mu\text{-}SMe)_2]$.

Table III. Electrochemical[a] and ^1H NMR Data for the Isomers of $[Mo_2Cp_2(CO)_2(\mu\text{-}SMe)_2]$

isomer	solvent	$E^{1/2}_{red1}$, V/Fc	$E^{1/2}_{red2}$, V/Fc	$E_{p,ox}$, V/Fc
cis	CH_3CN	−1.77	−2.19	−0.23
	thf	−1.90	−2.47	−0.12
trans–syn	CH_3CN	−1.91	−2.25	−0.10
trans–anti	CH_3CN	−1.95	−2.26	−0.07

isomer	^1H NMR,[b] δ (ppm)
cis	unstable, no spectroscopic data available
trans–syn	Cp: 5.43, 5.27 SMe: 2.33
trans–anti	Cp: 5.38 SMe: 2.26

[a] *E* from cyclic voltammetry measurements $\upsilon = 0.2$ V s^{-1}. [b] In $CDCl_3$.

(ii) The chemical syntheses[11,18] of *trans*-$[Mo_2Cp_2(CO)_2(\mu\text{-}SMe)_2]$ yield a mixture of separable isomers with distinct ^1H NMR characteristics and almost identical redox potentials (Table III). These were formulated as the trans–syn (2 Cp resonances) and the trans–anti (1 Cp resonance) forms of $[Mo_2Cp_2(CO)_2(\mu\text{-}SMe)_2]$.[18] The potentials of these stable isomers are quite different from the detection potential of the intermediate I (Table III).

On the basis of ^1H NMR data, Curtis[23] attributed the cis geometry to that isomer of $[Mo_2Cp_2(CO)_2(\mu\text{-}SMe)_2]$ showing a single Cp resonance (Cp 5.39; SMe 2.29; compare with the ^1H NMR data of the trans–anti isomer in Table III). However, our assignment is quite consistent with that reported very recently by Shaver[24] for $[W_2Cp_2(CO)_2(\mu\text{-}SCHMe_2)_2]$, for which a trans–anti configuration was established by X-ray crystallography and whose ^1H NMR spectrum displays a singlet for the Cp protons.

Accordingly, we believe that the isolable isomers of $[Mo_2Cp_2(CO)_2(\mu\text{-}SMe)_2]$ are correctly assigned as shown in Table III and that the intermediate I is *cis*-$[Mo_2Cp_2(CO)_2(\mu\text{-}SMe)_2]$.

4. CO-Catalyzed Cis/Trans Isomerization of $[Mo_2Cp_2(CO)_2(\mu\text{-}SMe)_2]$. The cis/trans isomerization of $[Mo_2Cp_2(CO)_2(\mu\text{-}SMe)_2]$, which requires the 180° rotation of one {MoCp(CO)} fragment with respect to the other, is slow under an inert atmosphere: the trans is formed on the electrolysis time scale. However, the isomerization process is *catalyzed by carbon monoxide*, as shown by the CV of 1 (Figure 3a), 2, or 3 run in the presence of CO: the redox processes of *cis*-$[Mo_2Cp_2(CO)_2(\mu\text{-}SMe)_2]$ (Figure 3a

(22) The fully detailed EHMO calculations carried out on the complexes *cis*- and *trans*-$[Mo_2Cp_2(CO)_2(\mu\text{-}SH)_2]$ and $[Mo_2Cp_2(CO)_2(\mu\text{-}SH)_3]^+$ will be reported later: El Khalifa, M.; Gloaguen, F.; Pétillon, F. Y.; Saillard, J. Y.; Talarmin, J. Work in progress.

(23) Li, P.; Curtis, M. D. *Inorg. Chem.* **1990**, *29*, 1242.

(24) Shaver, A.; Soo Lum, B.; Bird, P.; Livingstone, E.; Schweitzer, M. *Inorg. Chem.* **1990**, *29*, 1832.

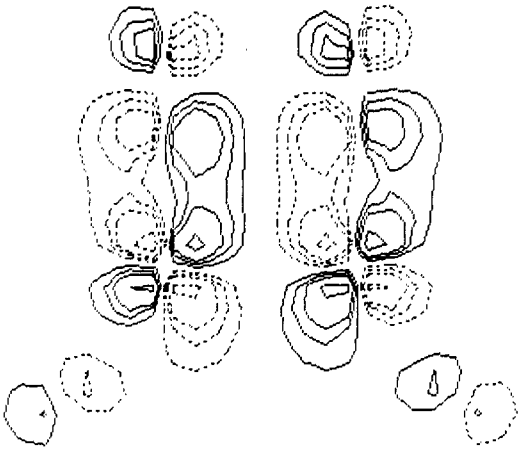

Figure 4. Contours of the LUMO of the model *cis*-$[Mo_2Cp_2(CO)_2(\mu\text{-}SH)_2]$ plotted in the (CO)MoMo(CO) symmetry plane. (The CO ligands are above the Mo–Mo vector.)

(broken line)) are replaced by those of the trans isomer (Figure 3a (solid line)) when CO is present.

EHMO calculations on the cis–syn and the trans–anti isomers of the model $[Mo_2Cp_2(CO)_2(\mu\text{-}SH)_2]$ and on their interactions with CO have been undertaken.[22] These calculations show that a typical feature of both MO diagrams is the presence of a rather low lying LUMO, situated in the middle of a large energy gap. A plot of the LUMO of the cis isomer is given in Figure 4. It is clear that, because of its low energy, this orbital is expected to be strongly involved in the interaction with the incoming CO. In the case of the cis isomer it has perfect symmetry and spatial localization for a strong interaction with one of the π^* orbitals of a CO approaching in a bridging position (Figure 4). The resulting *cis*-$[Mo_2Cp_2(CO)_2(\mu\text{-}CO)(\mu\text{-}SR)_2]$ complex, with a large HOMO–LUMO gap of 1.8 eV,[22] appears stable enough to be considered as a possible intermediate rather than a transition state in the reaction process of Scheme I. Therefore, we suggest that the catalytic effect arises from the insertion of CO into the Mo=Mo double bond, followed by a fast rearrangement of the resulting $[Mo_2Cp_2(CO)_2(\mu\text{-}CO)(\mu\text{-}SMe)_2]$ species (Scheme I).

The unstability of tricarbonyl species, e.g. $[Mo_2Cp_2(CO)_3(\mu\text{-}SMe)_2]$ and/or $[Mo_2Cp_2(CO)_2(\mu\text{-}CO)(\mu\text{-}SMe)_2]$, is confirmed by the fact that the two-electron reduction of other Mo(III) complexes, e.g. *cis*-$[Mo_2Cp_2(CO)_3(MeCN)(\mu\text{-}SMe)_2]^{2+}$[20] and $[Mo_2Cp_2(CO)_3(X)(\mu\text{-}SMe)_2]^+$ (X = Br, I),[22] leads to the rapid formation of *trans*-$[Mo_2Cp_2(CO)_2(\mu\text{-}SMe)_2]$ (CV time scale) via an unstable tricarbonyl species.[12] The nature of the possible intermediates involved in the reduction of these monosubstituted complexes will be investigated by EHMO calculations.[22]

II. Reactivity of *cis*- and *trans*-$[Mo_2Cp_2(CO)_2(\mu\text{-}SMe)_2]$ toward Isocyanide Ligands. 1. Electrochemical Reduction of 1–3 in the Presence of RNC (R = *t*-Bu, –CH_2Ph (=Bz), 2,6-diMePh (=xyl)). The reactivity of *cis*-$[Mo_2Cp_2(CO)_2(\mu\text{-}SMe)_2]$ described in section I.4 is not restricted to CO but extends to other π-accepting ligands such as RNC.

The effect of RNC on the CV of **1–3** is similar to that of CO: the redox processes of *cis*-$[Mo_2Cp_2(CO)_2(\mu\text{-}SMe)_2]$ are replaced by new reduction and oxidation peaks, at potentials depending on R, indicative of the formation of complexes with the RNC ligands. That these new compounds arise from the reaction of *cis*-$[Mo_2Cp_2(CO)_2(\mu\text{-}SMe)_2]$ with the isocyanide ligands is confirmed by the presence of isopotential points (IPP) on the CV curves

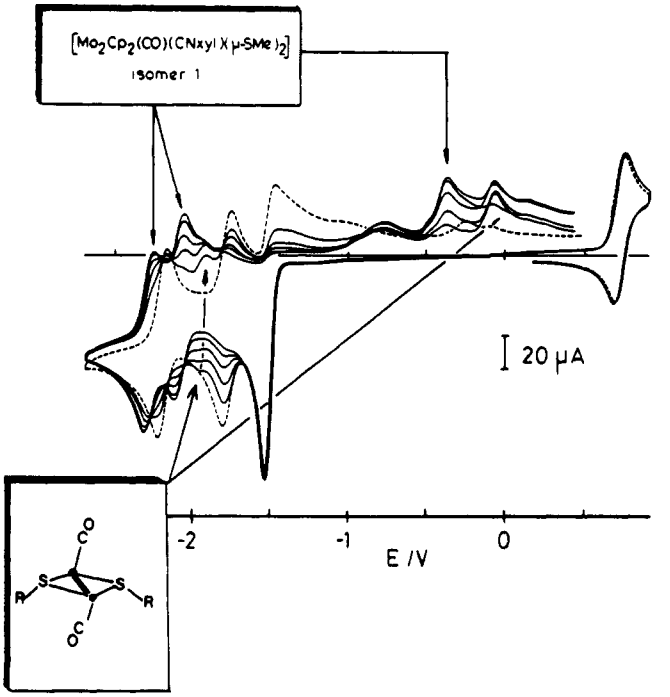

Figure 5. Cyclic voltammetry of a 1.7 mM solution of $[Mo_2Cp_2(CO)_2(\mu\text{-}SMe)_3]^+$ (**1**) in the absence (---) and in the presence (—) of increasing amounts of XylNC (0.1–0.7 equiv) (MeCN–0.1 M Bu_4NPF_6; vitreous carbon electrode; scan rate 0.2 V s^{-1}).

Table IV. Redox Potentials[a] of the $[Mo_2Cp_2(CO)_2(CNR)(\mu\text{-}SMe)_2]$ Isomers

RNC	solvent	$E^{1/2}_{red1}$, V/Fc	$E_{p,red2}$, V/Fc	$E_{p,ox}$, V/Fc
		Isomer 1		
xylNC	CH_3CN	−2.08	−2.28[b]	−0.38
	thf	−2.22	−2.43[b]	−0.41
t-BuNC	CH_3CN	−2.13	−2.45	−0.56, −0.44
	thf	−2.31	−2.56	−0.35, −0.50
BzNC	CH_3CN	−2.07	−2.39	−0.43
	thf	−2.22	−2.52	−0.43, −0.51
		Isomer 2		
xylNC	CH_3CN	−2.10	−2.29[b]	−0.25
	thf	−2.22	−2.46[b]	−0.34
t-BuNC	CH_3CN	−2.30[c]	−2.42	−0.35
	thf	−2.40[c]	−2.60	−0.27
BzNC	CH_3CN	−2.12[c]	−2.36	−0.39
	thf	−2.35[c]	−2.53	−0.33, −0.47

[a] E from cyclic voltammetry v = 0.2 V s^{-1}. [b] $E^{1/2}_{red2}$. [c] $E_{p,red1}$.

obtained in the presence of increasing amounts of the ligand (Figure 5, R = xyl, complex **1**): this demonstrates that *cis*-$[Mo_2Cp_2(CO)_2(\mu\text{-}SMe)_2]$ is converted to a product (see isomer 1 in Table IV) and that side reactions are unimportant on this time scale[25-27] (however, see section II.3). Similar curves were obtained for the other isocyanides (R = *t*-Bu, Bz) as well as with complexes **2** and **3**.

Controlled-potential electrolyses carried out at $E_{p,red1}$ in the presence of RNC lead to different results depending on the nature of R.

In the presence of xylNC the coulometric n value is close to 2 F/mol of complex for the electrolyses of **2** and

(25) Gaudiello, J. G.; Wright, T. C.; Jones, R. A.; Bard, A. J. *J. Am. Chem. Soc.* **1985**, *107*, 888.
(26) (a) Dietrich, M.; Heinze, J.; Fisher, H.; Neugebauer, F. A. *Angew. Chem., Int. Ed. Engl.* **1986**, *25*, 1021. (b) Hinkelmann, K.; Mahlendorf, F.; Heinze, J.; Schacht, H. T.; Field, J. S.; Vahrenkamp, H. *Angew. Chem., Int. Ed. Engl.* **1987**, *26*, 352.
(27) Fitch, A.; Edens, G. J. *J. Electroanal. Chem.* **1989**, *267*, 1.

Table V. Spectroscopic Data for the Isomers of $[Mo_2Cp_2(CO)(CNR)(\mu\text{-}SMe)_2]$

RNC	^{1}H NMR,[a] δ (ppm)	IR, cm^{-1}
	Isomer 1	
xylNC	Cp: 5.24, 4.98 SMe: 2.27 xyl: 6.94, 2.15	
t-BuNC	Cp: 5.21, 5.15 SMe: 2.33 *t*-Bu: 1.15	
BzNC	Cp: 5.14, 4.81 SMe: 2.21 Bz: 7.30, 4.60	
	Isomer 2	
xylNC	Cp: 5.36, 5.03 SMe: 2.21 xyl: 6.94, 2.15	CO: 1825 CN: 2020, 1990[b]
t-BuNC	Cp: 5.32, 4.80 SMe: 2.18 *t*-Bu: 1.26	CO: 1815 CN: 2080, 2045[c]
BzNC	Cp: 5.31, 4.91 SMe: 2.12 Bz: 7.30, 4.75	CO: 1825 CN: 2060[b]

[a] Solvent $CDCl_3$. [b] Solvent $CDCl_3$. [c] Solvent CH_2Cl_2.

3 carried out in the presence of 1 equiv of ligand in a thf or a MeCN electrolyte. As we noted in the absence of ligand, the reduction of 1 in the presence of xylNC (1 equiv) is completed after 1.3 F/mol of complex (thf electrolyte) or 1.4–2 F/mol of complex (MeCN electrolyte) have been consumed. Again, the reduction of 1 by the SMe^- anion released in the medium must take part to effect the overall process.

The reduction potentials of the product formed on reducing 1 in the presence of xylNC corresponds to those detected by CV before electrolysis. By contrast, two irreversible overlapping oxidation peaks are observed instead of one before electrolysis. The yield in the xylNC complex, calculated by comparing the first reduction peak current of the product (one-electron reduction) to the oxidation peak current of 1 before electrolysis is close to 80%.

In the Presence of *t*-BuNC or BzNC. The electrolyses performed in the presence of *t*-BuNC (5 equiv) or BzNC (2 equiv) result in the formation of a mixture of products. One of these is the complex observed by CV before electrolysis. The electrolyses of 1 in a thf medium containing *t*-BuNC (5 equiv) or BzNC (1–2 equiv) require 1.3 F/mol of complex, whereas 1.7 ± 0.2 F/mol are consumed for the same reaction in a MeCN electrolyte. We were not able to calculate the yield of complex by cyclic voltammetry due to the difficulties of measuring peak currents for overlapping processes.

2. Characterization of the Isocyanide Complexes. ^{1}H NMR spectra of the crude products extracted from the catholyte demonstrate that two isomers are formed during the electrolyses; they possess two nonequivalent Cp rings, two equivalent MeS, and one RNC ligand (Table V). The presence of a broad band at 1815–1825 cm^{-1}, assigned to a ν_{CO}, indicates that the complexes retain a carbonyl group. The isomers can therefore be formulated as $[Mo_2Cp_2(CO)(CNR)(\mu\text{-}SMe)_2]$, and this is confirmed by the presence of the corresponding molecular ion peak on the mass spectra (see Experimental Section).

3. Mechanism of the Formation of the Isocyanide Complexes. The isomer detected by CV of complexes 1–3 in the presence of RNC (isomer 1 in Tables IV and V) clearly arises from the reaction of *cis*-$[Mo_2Cp_2(CO)_2(\mu\text{-}SMe)_2]$ with the isocyanide ligand (Figure 5). The second isomer (isomer 2, Tables IV and V), formed more slowly on the electrolysis time scale, results from the reaction of

Scheme III[a]

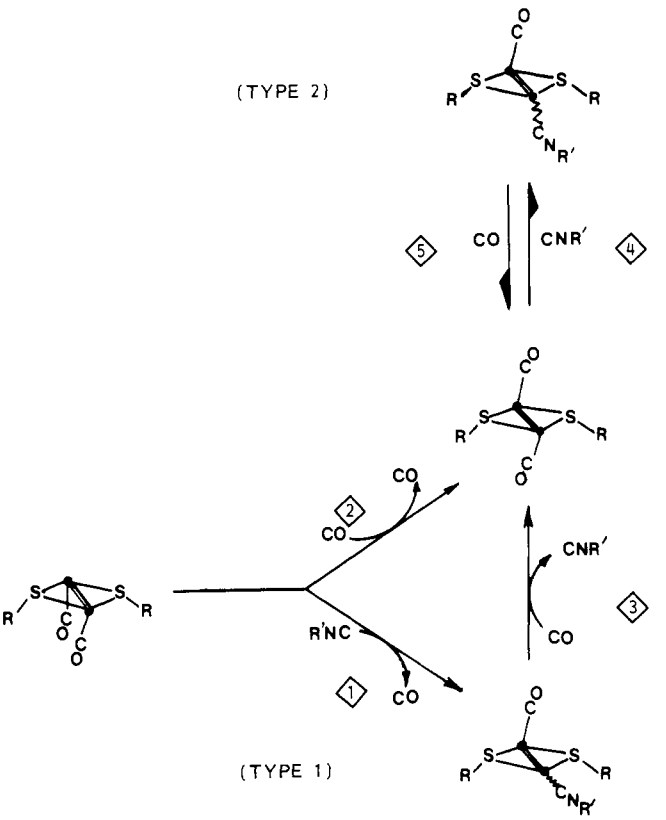

[a] R = Me; R' = *t*-Bu, xyl, Bz. ● = Mo–Cp.

trans-$[Mo_2Cp_2(CO)_2(\mu\text{-}SMe)_2]$ with RNC. Our evidence for this novel reaction is as follows.

The binding of RNC to *cis*-$[Mo_2Cp_2(CO)_2(\mu\text{-}SMe)_2]$, which occurs probably according to a pathway similar to that described for CO in Scheme I, leads to the release of a carbonyl group (Scheme III, step 1). This reaction triggers the cis/trans isomerization of $[Mo_2Cp_2(CO)_2(\mu\text{-}SMe)_2]$ (Scheme III, step 2): the formation of the trans isomer, not detected by CV in the absence of ligand, is observed when the CV is run in the presence of RNC (Figure 5). The reaction of RNC with *trans*-$[Mo_2Cp_2(CO)_2(\mu\text{-}SMe)_2]$ eventually produces isomer 2 of $[Mo_2Cp_2(CO)(CNR)(\mu\text{-}SMe)_2]$ (Scheme III, step 4). The occurrence of the latter step has been confirmed by reacting an authentic sample of *trans*-$[Mo_2Cp_2(CO)_2(\mu\text{-}SMe)_2]$ with the isocyanides: the electrochemical and spectroscopic characteristics of the product correspond to those of one of the complexes (isomer 2, Tables IV and V) produced during the electrolyses. The isocyanides xylNC and BzNC react faster than *t*-BuNC, which suggests the limitation by a steric factor.

It is therefore clear that the CO released on RNC binding to *cis*-$[Mo_2Cp_2(CO)_2(\mu\text{-}SMe)_2]$ plays a crucial part in the formation of isomer 2. When the CO is removed from the solution during the electrolysis of 1 in the presence of RNC, e.g. by strong N_2 bubbling, then the formation of isomer 1 is favored. This is illustrated in Figure 6a where the yield in isomer 1 (R = *t*-Bu) is close to 80%, as measured by CV. Similar results are obtained with BzNC (yield 75–80%). However, although N_2 is bubbled through the solution during the course of the electrolysis, some isomer 2 is present: ^{1}H NMR analysis of the products extracted from the catholyte shows that the ratio of isomers 1 and 2 does not exceed 3/1.

Carbon monoxide can displace the RNC ligand from both isomers of $[Mo_2Cp_2(CO)(CNR)(\mu\text{-}SMe)_2]$ to generate

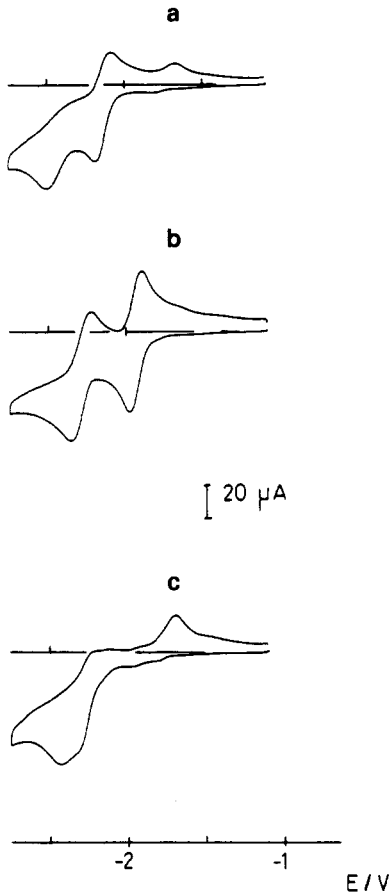

Figure 6. Cyclic voltammetry of the product obtained (a) after controlled-potential electrolysis under vigourous N_2 bubbling of a 1.6 mM solution of $[Mo_2Cp_2(CO)_2(\mu\text{-}SMe)_3]^+$ (1) in the presence of 5 equiv *t*-BuNC, (b) after CO bubbling of the solution in (a), (c) after flushing the solution in (b) with N_2 (MeCN–0.1 M Bu_4NPF_6; vitreous carbon electrode; scan rate 0.2 V s^{-1}).

trans-$[Mo_2Cp_2(CO)_2(\mu\text{-}SMe)_2]$ (Scheme III, steps 3 and 5): this is illustrated by the CV in Figure 6b run after CO was bubbled through a solution containing mainly isomer 1 (Figure 6a). Removal of CO from the solution in Figure 6b (N_2 bubbling) generates isomer 2 only (Figure 6c); the formation of the latter is reversible (Scheme III, steps 4 and 5) whereas isomer 1 cannot be regenerated once the RNC ligand has been displaced from this complex. The reaction sequence illustrated in Figure 6a–c (R = *t*-Bu) is thus an example of a *CO-induced isomerization*.

Two types of isomerism may be envisaged for $[Mo_2Cp_2(CO)(CNR)(\mu\text{-}SMe)_2]$, based on the cis/trans arrangement of the CO and RNC ligands and on the geometry (linear vs bent or semibridging) of the RNC ligand. The fact that CO and RNC have similar effects on the CV of *cis*-$[Mo_2Cp_2(CO)_2(\mu\text{-}SMe)_2]$ suggests that the reaction products, e.g. *trans*-$[Mo_2Cp_2(CO)_2(\mu\text{-}SMe)_2]$ and isomer 1 of $[Mo_2Cp_2(CO)(CNR)(\mu\text{-}SMe)_2]$, have similar, i.e. trans, geometries.

This aspect of our work is currently under investigation, and attempts to grow crystals of isomers 1 and 2 suitable for an X-ray structural determination are in progress.

Conclusion

The electrochemical reduction of the Mo(III) dinuclear complexes $[Mo_2Cp_2(CO)_2(\mu\text{-}SMe)_3]^+$ (1), $[Mo_2Cp_2(CO)_2(Cl)_2(\mu\text{-}SMe)_2]$ (2), and $[Mo_2Cp_2(CO)_2(Br)_2(\mu\text{-}SMe)_2]$ (3) generates the reactive intermediate *cis*-$[Mo_2Cp_2(CO)_2(\mu\text{-}SMe)_2]$. This species undergoes (i) a slow cis/trans isomerization under an inert atmosphere in the absence of ligand, (ii) a fast cis/trans isomerization in the presence of CO, and (iii) a fast substitution reaction leading to $[Mo_2Cp_2(CO)(CNR)(\mu\text{-}SMe)_2]$, when generated in the presence of isocyanide.

The theoretical calculations are in very good agreement with the experimental results summarized in Scheme I, and they provide a rationale for the high reactivity of the intermediate: this is due to the accessibility of the low-lying LUMO of I, which has a symmetry perfectly adapted to interact with CO and RNC ligands.

The reactivity of the $[Mo_2Cp_2(CO)(L)(\mu\text{-}SMe)_2]$ complexes (L = CO or RNC) is illustrated in Scheme III: two isomers of $[Mo_2Cp_2(CO)(CNR)(\mu\text{-}SMe)_2]$ are formed on reacting *cis*- and *trans*-$[Mo_2Cp_2(CO)_2(\mu\text{-}SMe)_2]$ with isocyanides; on the other hand, the coordinated RNC are readily released from both isomers of the substituted complexes in the presence of carbon monoxide, but only *trans*-$[Mo_2Cp_2(CO)_2(\mu\text{-}SMe)_2]$ is formed.

Experimental Section

Methods and Materials. All the experiments were carried out under N_2 or Ar, using Schlenk techniques for the syntheses. Tetrahydrofuran (thf) and CH_2Cl_2 were purified as described previously.[9] Acetonitrile (Prolabo HPLC grade) was used without purification. The supporting electrolyte $[Bu_4N][PF_6]$ was prepared by titration of $H(PF_6)$ with $[Bu_4N][OH]$ and purified as described previously.[9] The isocyanides (*tert*-butyl isocyanide (*t*-BuNC), 2,6-dimethylphenyl isocyanide (xylNC) (Fluka); benzyl isocyanide (BzNC) (Aldrich)) were used as received. The complexes $[Mo_2Cp_2(CO)_2(\mu\text{-}SMe)_3]^+$ (1), $[Mo_2Cp_2(CO)_2(Cl)_2(\mu\text{-}SMe)_2]$ (2), $[Mo_2Cp_2(CO)_2(Br)_2(\mu\text{-}SMe)_2]$ (3), and *trans*-$[Mo_2Cp_2(CO)_2(\mu\text{-}SMe)_2]$ were prepared according to published procedures.[11,18] The ^1H NMR spectra were obtained on a JEOL C 60 HL or a JEOL FX 100 or a BRUKER AC 300 spectrophotometer and were referenced to Me_4Si. The IR spectra were recorded on a Pye-Unicam SP 2000 machine. The mass spectra were obtained on a GC/MS Hewlett-Packard 5995C apparatus.

Electrochemistry. The electrochemical equipment (apparatus, cells, set of electrodes) was as described previously.[9] Ferrocene was added as an internal standard at the end of the experiments, and the potentials (text, tables, figures) are referenced to the ferrocene/ferrocenium ion couple.

Computational Details. All the calculations have been made within the extended Hückel formalism,[28] using the weighted H_{ij} formula.[29] The atomic parameters are taken from the literature.[30] The bond distances and angles used in the calculations are taken from averaged experimental structures.[11,24,31]

Electrosyntheses of *trans*-$[Mo_2Cp_2(CO)_2(\mu\text{-}SMe)_2]$ and $[Mo_2Cp_2(CO)(CNR)(\mu\text{-}SMe)_2]$. Two types of electrolyses were performed (i) small-scale electrolyses (4–50 mg of starting material, 6×10^{-6}–9×10^{-5} mol) carried out on solutions of complexes 1–3 in the absence or in the presence of RNC (R = xyl, 1 equiv; R = Bz, 2 equiv; R = *t*-Bu, 5 equiv), were performed to calculate coulometric *n* values and the yields of *trans*-$[Mo_2Cp_2(CO)_2(\mu\text{-}SMe)_2]$ or $[Mo_2Cp_2(CO)(CNR)(\mu\text{-}SMe)_2]$ (isomer 1), respectively. The yields were obtained from CV experiments by comparing the first reduction peak current of the product ($i_{p,red1}(P)$) to the first oxidation peak current of the starting material before electrolysis ($i_{p,ox1}$). Both systems correspond to one-electron processes, and the diffusion coefficients of the product and of the starting material are assumed to be identical. Under these conditions, yield = $[i_{p,red1}(P)/i_{p,ox1}] \times 100$.

(ii) Larger scale electrolyses (100–200 mg of starting material, 0.2–0.4 mmol) intended to isolate and characterize the reduction products were carried out mostly with complex 1. The procedures

(28) (a) Hoffmann, R.; Lipscomb, W. N. *J. Chem. Phys.* **1962**, *36*, 2179. (b) Hoffmann, R. *J. Chem. Phys.* **1963**, *39*, 1399.
(29) Ammeter, J. M.; Bürgi, H. B.; Thibeault, J. C.; Hoffmann, R. *J. Am. Chem. Soc.* **1978**, *100*, 3686.
(30) El Khalifa, M.; Pétillon, F. Y.; Saillard, J. Y.; Talarmin, J. *Inorg. Chem.* **1989**, *28*, 3849.
(31) Benson, I. B.; Killops, S. D.; Knox, S. A. R.; Welch, A. J. *J. Chem. Soc., Chem. Commun.* **1980**, 1137.

for the electrosyntheses of *trans*-$[Mo_2Cp_2(CO)_2(\mu\text{-}SMe)_2]$ and of $[Mo_2Cp_2(CO)(CNR)(\mu\text{-}SMe)_2]$ were as described below.

***trans*-$[Mo_2Cp_2(CO)_2(\mu\text{-}SMe)_2]$.** A solution of complex 1 in a thf–0.2 M $[Bu_4N][PF_6]$ or a MeCN–0.1 M $[Bu_4N][PF_6]$ electrolyte was reduced on a Hg-pool cathode at −1.6 V under N_2 or Ar. The initial dark orange solution turned brown as the experiment proceeded. When the cell current had decayed to the background level, the catholyte was syringed out of the electrochemical cell, transferred into a Schlenk flask under N_2, and taken down to dryness. The residue (product + supporting electrolyte) was extracted four times with ca. 10 mL of pentane, the filtrates were collected in a flask, and the solvent was removed under vacuum. ^1H NMR analysis of the crude product showed the presence of *trans*-$[Mo_2Cp_2(CO)_2(\mu\text{-}SMe)_2]$ and of trace amounts of supporting electrolyte. The mass spectrum showed ions corresponding to $[M]^+$ (*m/e* 472), $[M - CO]^+$ (*m/e* 444), $[M - 2CO]^+$ (*m/e* 416), $[M - 2CO\text{-}2(CH_3)]^+$ (*m/e* 386), $[M - 2CO - 2(CH_3) - C_5H_5]^+$ (*m/e* 321), and $[M - 2CO - 2(CH_3) - 2(C_5H_5)]^+$ (*m/e* 256).

$[Mo_2Cp_2(CO)(CNR)(\mu\text{-}SMe)_2]$. The same procedure as described above was followed, except that isocyanide RNC (R = xyl, 1 equiv; R = Bz, 2 equiv; R = *t*-Bu, 5 equiv) was added to the solution of complex 1. After the workup of the brown to greenish brown catholyte, ^1H NMR spectroscopy showed the presence of two isomers of the product. Column chromatography on silica gel or Florisil did not allow a proper separation of the isomers, which also underwent some decomposition on the column. In order to favor the formation of isomer 1, a vigorous bubbling of N_2 was maintained through the solution of complex 1 and RNC while the electrolysis was proceeding (see Results). A green solution resulted from the experiments performed under these conditions. After a workup similar to that described for *trans*-$[Mo_2Cp_2(CO)_2(\mu\text{-}SMe)_2]$, ^1H NMR analysis of the product showed that the ratio of isomer 1 to isomer 2 had increased, with a maximum of 3/1.

R = xyl. Anal. Calcd for $[Mo_2Cp_2(CO)(CNxyl)(\mu\text{-}SMe)_2]\cdot CH_2Cl_2$ ($Mo_2C_{23}H_{27}NS_2OCl_2$): C, 41.8; H, 4.1; N, 2.1;, Mo, 29.1. Found: C, 41.5; H, 4.6; N, 2.2; Mo, 29.8. The mass spectrum showed ions corresponding to $[M]^+$ (*m/e* 575), $[M - (CH_3)]^+$ (*m/e* 560), $[M - (CH_3) - (CO)]^+$ (*m/e* 532), $[M - (CO) - (xylNC)]^+$ (*m/e* 416), $[M - (CO) - (xylNC) - 2(CH_3)]^+$ (*m/e* 386), $[M - (CO) - (xylNC) - 2(CH_3) - (C_5H_5)]^+$ (*m/e* 321), and $[M - (CO) - (xylNC) - 2(CH_3) - 2(C_5H_5)]^+$ (*m/e* 256).

R = *t*-Bu. The mass spectrum showed ions corresponding to $[M]^+$ (*m/e* 527), $[M - (CO)]^+$ (*m/e* 499), $[M - (t\text{-Bu})]^+$ (*m/e* 470), $[M - (CO) - (t\text{-BuNC})]^+$ (*m/e* 416), $[M - (CO) - (t\text{-BuNC}) - (CH_3)]^+$ (*m/e* 401), $[M - (CO) - (t\text{-BuNC}) - 2(CH_3)]^+$ (*m/e* 386), $[M - (CO) - t\text{-BuNC}) - 2(CH_3) - (C_5H_5)]^+$ (*m/e* 321), $[M - (CO) - (t\text{-BuNC}) - 2(CH_3) - 2(C_5H_5)]^+$ (*m/e* 256).

R = BzNC. The mass spectrum showed peaks corresponding to $[M]^+$ (*m/e* 561), $[M - (CO)]^+$ (*m/e* 533), $[M - (BzNC)]^+$ (*m/e* 444), and $[M - (CO) - (BzNC) - 2(CH_3)]^+$ (*m/e* 386).

Acknowledgment. The CNRS (Centre National de la Recherche Scientifique) is acknowledged for financial support to this work.

Crystal and Molecular Structure of an Asymmetric Hydrogenation Catalyst–Substrate Adduct, Δ-Bis(tiglato){(*R*)-2,2′-bis(diphenylphosphino)-1,1′-binaphthyl}-ruthenium(II), $[Ru^{II}(BINAP)(O_2CCMe{=}CHMe)_2]$

Michael T. Ashby* and Masood A. Khan

Department of Chemistry, University of Oklahoma, 620 Parrington Oval, Room 208, Norman, Oklahoma 73019

Jack Halpern*

Department of Chemistry, The University of Chicago, Chicago, Illinois 60637

Received October 25, 1990

The molecular structure of an active catalyst in the homogeneous asymmetric hydrogenation of tiglic acid has been determined by single-crystal X-ray crystallography. Bis(tiglato){(*R*)-2,2′-bis(diphenylphosphino)-1,1′-binaphthyl}ruthenium(II), (*R*)-**1b**, crystallizes in the monoclinic space group $P2_1$ with $Z = 2$, $a = 12.709$ (5) Å, $b = 15.622$ (5) Å, $c = 11.289$ (5) Å, $\beta = 99.43$ (4)°, $R = 0.021$, and $R_w = 0.027$. The tiglate ligands are η^2-carboxylate-bound. The configuration at the metal is Δ, and the conformation of the seven-membered chelate ring is λ. No bonding interactions between the C=C bonds of the substrates and the metal center are found in the solid state. The coordination environment of the Ru atom in **1b** in the solid state is essentially the same as that in noncoordinating solvents, as deduced by NMR spectroscopy. These results are consistent with the conclusion, on the basis of kinetic measurements previously reported, that if coordination of the C=C bond to Ru is a prerequisite to insertion into a Ru–H bond, then such coordination must occur after reaction with H_2.

We have recently reported the results of a study of the kinetics and mechanism of asymmetric hydrogenation of α,β-unsaturated carboxylic acids, catalyzed by ruthenium complexes derived from the precursor bis(acetato){(*R*)- or (*S*)-2,2′-bis(diphenylphosphino)-1,1′-binaphthyl}ruthenium(II) ($[Ru^{II}(BINAP)(OAc)_2]$, **1a**).[1] The results of this study, conducted in methanol solution, suggested a mechanism involving: (1) rapid equilibrium between **1** and

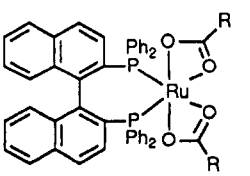

R = CH_3 (**1a**)
R = $C(CH_3){=}CHCH_3$ (**1b**)
R = $C(CH_3)_3$ (**1c**)

the substrate, (2) heterolytic splitting of H_2 to give a ruthenium–dicarboxylate–monohydride species, (3) insertion

(1) (a) Ashby, M. T.; Halpern, J. *J. Am. Chem. Soc.* **1991**, *113*, 589. (b) For a general review of asymmetric catalysis by BINAP complexes, see: Noyori, R.; Takayi, H. *Acc. Chem. Res.* **1990**, *23*, 345.

0276-7333/91/2310-2011$02.50/0